Microfluidic channel structures speed up mixing of multiple emulsions by a factor of ten

Kevin J. Land, Mesuli Mbanjwa, and Jan G. Korvink

Citation: Biomicrofluidics **8**, 054101 (2014); doi: 10.1063/1.4894498
View online: http://dx.doi.org/10.1063/1.4894498
View Table of Contents: http://scitation.aip.org/content/aip/journal/bmf/8/5?ver=pdfcov
Published by the AIP Publishing

Microfluidic channel structures speed up mixing of multiple emulsions by a factor of ten

Kevin J. Land,[1,2,a)] Mesuli Mbanjwa,[1,3] and Jan G. Korvink[2]
[1]*Council for Scientific and Industrial Research (CSIR), Meiring Naude Road, Pretoria, South Africa*
[2]*Department of Microsystems Engineering (IMTEK), University of Freiburg, Georges-Köhler-Allee 103, Freiburg 79110, Germany*
[3]*University of Witwatersrand, Johannesburg, South Africa*

(Received 20 June 2014; accepted 22 August 2014; published online 2 September 2014)

We present a novel use for channel structures in microfluidic devices, whereby two two-phase emulsions, one created on-chip, the other off-chip, are rapidly mixed with each other in order to allow for the coalescence of one emulsion with the other. This approach has been motivated by the difficulty in introducing aqueous cross linking agents into droplets by utilising conventional approaches. These conventional approaches include continuous introduction of the different aqueous reagents before droplet formation or alternatively formation of individual droplets of each reagent and subsequent droplet merging later in the microfluidic device. We show that our approach can decrease the mixing time for these fluidic systems by a factor greater than 10 times when compared to a standard microfluidic channel without structures, thereby also allowing for additional reaction time within the microfluidic device. This method shows an application for microfluidic channel structures not before demonstrated, also demonstrating an alternative method for introducing reagents such as cross linkers which link polymer chains to form particles, and provides an example where enzymes are immobilized in monodisperse particles. © *2014 AIP Publishing LLC*. [http://dx.doi.org/10.1063/1.4894498]

I. INTRODUCTION

Due to the nature of flows in microfluidic channels, it is difficult to mix fluids. Typically, flow is laminar, and mixing occurs by diffusion, which is very slow compared to mixing in turbulent flows. The Reynold's number, $\mathrm{Re} = \rho \mathrm{VL}/\eta$, where ρ is the fluid density, V is the linear velocity, L is the system characteristic length, and η is the viscosity, gives an indication of the degree of dominance of inertial to viscous forces. In most microfluidic systems, the viscous forces dominate, leading to low Reynold's numbers and laminar flow. In the current work, it is also expected that viscous forces will dominate both for the flow of continuous phase oil and pre-emulsion. It is critical, both for increasing system throughput and complete mixing, to overcome these limitations. Many methods to achieve this have been proposed and studied, and a number of reviews give a complete overview of the methods and the main issues associated with mixing at the microscale.[1–3] *Active mixing*, which is usually defined as mixing by the addition of an external energy supply, utilises a number of activation methods, including acoustic,[4] ultrasonic,[5] electrokinetic,[6] thermal,[7] and magnetic mixing.[8] *Passive mixing*, which is of interest in this work, typically takes the form of surface modifications in the device of interest, either by means of a topological or chemical change. Since passive mixing relies on diffusion and often is further driven by chaotic advection, designs are required which optimise the contact surface between the fluids to be mixed. Early designs made use of simple T- or Y-mixers.[9,10] Topological changes include splitting and recombining flow, either in two dimensional[11] or

a)Author to whom correspondence should be addressed. Electronic mail: kland@csir.co.za

three dimensional[12,13] designs, a modification of channel shapes such as the introduction of zig-zag patterns[14] and the fabrication of complex channels. Chemical methods involve selectively changing surface properties of regions of the channel surfaces in order to generate vortices (localised flow patterns) induced by differences in electrostatic potential.[15]

A particular passive mixer which has received attention[16–19] is one in which the channel surfaces are physically modified by the addition of grooves or rib-like structures. A special case of this is the so-called staggered herringbone mixer first proposed by Stroock *et al.*[20] Structurally, the mixer consists of a series of ridges patterned into the floor of the device. This mixer is easily manufactured with conventional lithography methods (a two-layer process), and results in rapid mixing by inducing transverse flows in the microfluidic channels. These types of mixers are primarily used for the mixing of continuous fluid flows. This work proposes to use these structures for the mixing of two separately generated emulsion streams, one of these being actively generated on the microfluidic device as a series of droplets. To avoid confusion, mixing is defined as the even distribution of the secondary emulsion stream throughout the channel volume, thus allowing for consistent contact with the larger emulsion droplets.

Droplet-based microfluidics has found application in many areas.[21,22] Biological and chemical reagents can be isolated within droplets, making them ideal micro reactor platforms. Droplet operations are highly repeatable and can be scaled, allowing for many different unit operations, such as splitting and recombining, to be performed. A toolbox of such operations has been developed and is excellently described in Kintses *et al.*[23] Droplets also allow for direct synthesis of particles and can also be utilised for direct encapsulation of biological or chemical species such as enzymes.[24,25]

Droplets are typically formed utilising either T-junction[26] or flow focussing[27] configurations. Typically, the reagents necessary for the reaction or process are added before droplet generation due to the difficulty of adding reagents after the droplet has been formed. These reagents are either premixed before introduction to the microfluidic chip or are introduced in a co-flowing arrangement.[28] Mixing is then accomplished within the droplets by chaotic advection, which is rapid and easily achieved. It is also possible to independently form droplets of the various reagents and join these subsequently in the microfluidic device. A number of schemes have been proposed to achieve this.[29–33] However, these methods typically only work for a limited range of flow parameters or require active control, for example, via electrical impulses.

In order to determine whether any of these well established methods would be viable, various experiments were performed, specifically studying whether all the necessary aqueous reagents (Figure 1(a), w_1, w_2, and w_3) could be introduced before droplet formation. This would

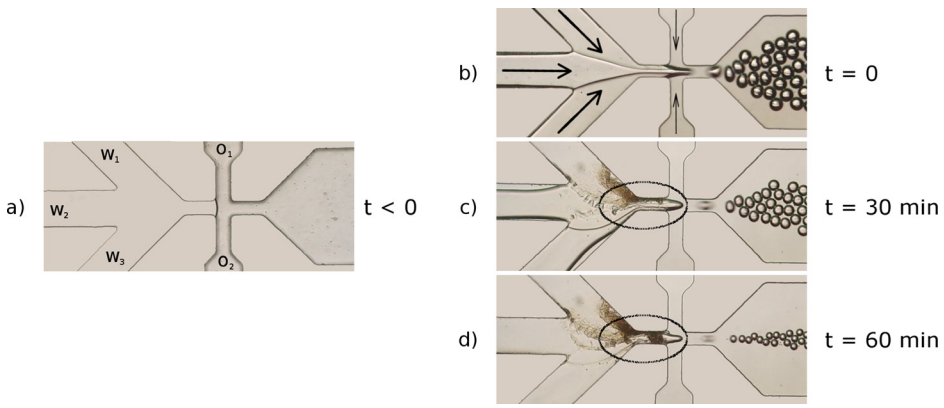

FIG. 1. Series of photographs showing the problem experienced when introducing reagents in continuous form. (a) shows the channels before the experiment starts, with w_1, w_2, w_3 representing water phase and o_1 and o_2 representing oil phase, (b) shows the start of the experiment, with arrows indicating the direction of fluid flow, while (c) and (d) show various stages of blocking in the channel. As blockage gets worse ((c) and (d)), droplet formation (frequency and size) decreases dramatically. Ellipse shows the region of worst blockage.

clearly be the most efficient solution. However, the cross linker (glutaraldehyde) utilised in these experiments to bond one polymer chain to another in order to form particles, also results in a very fast blockage of the droplet formation channel, with blockage clearly affecting flow after only 30 min (Figure 1(c)), rendering this standard method completely unusable.

Alternative methods were also investigated, shown in Figure 2, including the introduction of alternative thinner and wider channel regions and channel obstructions, but these also did not result in successful mixing of larger and smaller droplets.

More recently, herringbone and other topological structures inside micro channels have been suggested for micro vortex focusing and guiding of particles for the purpose of sorting based on size.[34,35]

The current work proposes to combine these two seemingly separate functions, namely, the merging of droplet emulsion streams and the focusing of these streams to effect mixing and separation of the droplets from the channel walls. The problem of low frequency droplet merging would be solved by this method, and additionally even mixing would be obtained.

We therefore present a method of utilising topological microstructures for the purpose of passively mixing two streams of emulsions, each contained in a common secondary phase. This introduces a new application for these structures where in the past they have typically been utilised for mixing of laminar single phase streams. This allows for the generation of droplets independently from the introduction of other reagents, and results in very rapid entry of these other reagents into the droplet when required. This also allows for time delays between the introduction of reagents. A number of different structures have been manufactured and tested, and an optimal structure for this purpose has been identified. A comparison is made between the mixing of these emulsions with and without structures, and the improvement gained in mixing efficiency, particle homogeneity, and mixing time is discussed.

This contribution would find application in many processes, but we show specifically the ability to externally add cross linker to an existing emulsion using a secondary emulsion. Specifically, the manufacture of self-immobilised enzyme particles is demonstrated to show practical use of the technique (see Section III).

II. SIMULATION, TESTING, AND DESIGN

A large variety of herringbone-like structures were designed and tested. These were initially chosen based on the most effective structures reported in the literature,[20] together with candidate structures where some of the basic parameters had been changed in order to determine whether they were optimal for the purposes of this work. Eight of these structures are shown in Figure 3, selected for their unique effect on the resulting flow.

Designed structure widths are 71 μm (p), except for (h) where the structure width is 134 μm. The designed distance between the ribs is 78 μm (q), except (g) where the distance is 141 μm. Flow simulations were performed using the software package SolidWorks Flow Simulation, which is an add-on to the standard SolidWorks engineering design software that solves time-dependent Navier-Stokes equations. In our case, we solve for single phase Stokes flow and use the software to visualise the flow trajectories of the various emulsions which have been introduced.

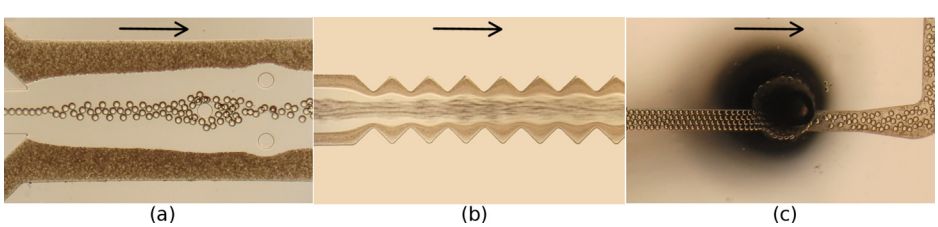

FIG. 2. Various experiments tried to force mixing of the pre-emulsion and the larger droplets (a) introduction of structures into the main channel, (b) constrictive side wall structures, and (c) introduction of the pre-emulsion from the top of the channel.

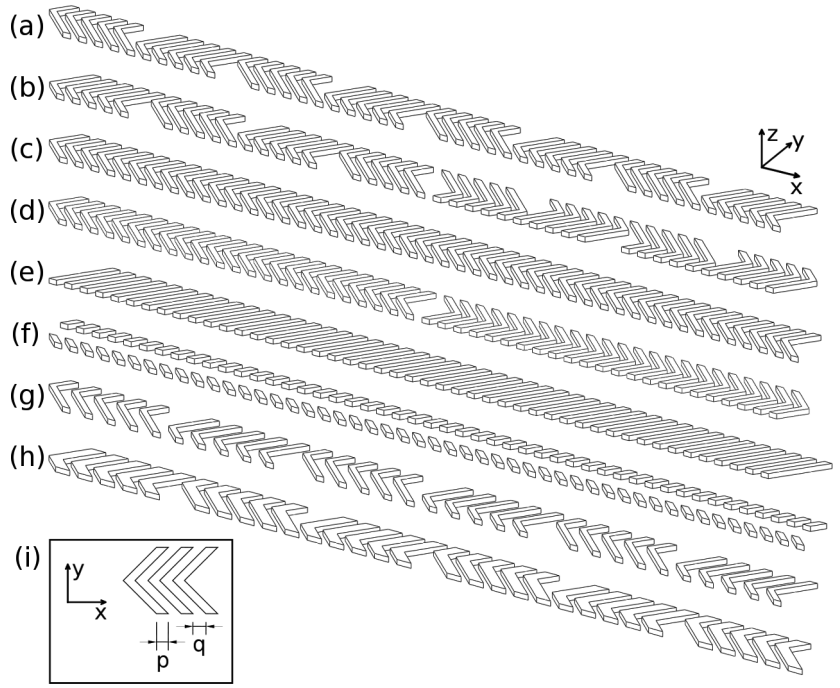

FIG. 3. Schematic showing the various structures tested. p is the structure width, while q shows the spacing between structures. Specific structures in text are referred to by their capitalised letter: (a) = A, (b) = B, etc.

Flow boundary conditions can be specified at all of the model openings. Inlets, defined as the three flow inlets marked in Figure 4 at junction B, are specified in terms of volume flow rate. Note that secondary emulsions enter from each side of the channel, while primary emulsion is in the centre of the channels. The single outlet is defined by atmospheric backpressure. Structures were simulated over a distance of 26 mm.

Fluid properties are defined as follows: densities of the oil and water phases are given by $\rho_o = 840\,\text{kg/m}^3$ and $\rho_w = 997\,\text{kg/m}^3$, respectively, while viscosities are given by $\eta_o = 0.03\,\text{Pa s}$ and $\eta_w = 0.001\,\text{Pa s}$, respectively. These are experimentally measured values for the continuous phases in the experiment and are directly used for the simulation.

Figure 5 shows select results of the simulations for the standard structures A, C, and E. It is interesting to note the different spatial flow trajectories which result from each of the structures. Structure C, for example, does not allow for any flow of secondary emulsion to cross the centre of the channel (C.5 green and blue secondary emulsions). Structure E allows for both secondary emulsions to cross the centre line, but the flow pattern does result in efficient mixing within the defined length of channel. Structure A, in turn, allows for some flow of secondary

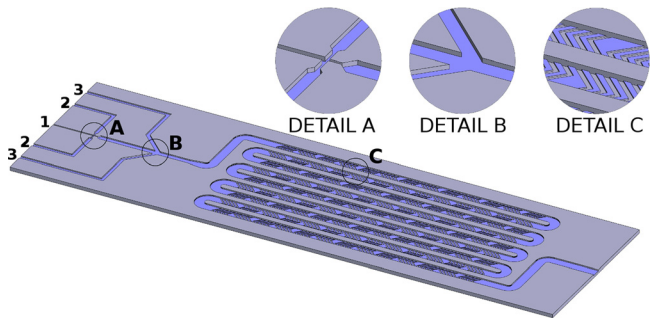

FIG. 4. Design of the microfluidic circuit showing the positioning of structures in the serpentine channel. Structure testing was done in straight channels, while comparative tests without structures were done in the serpentine channel shown.

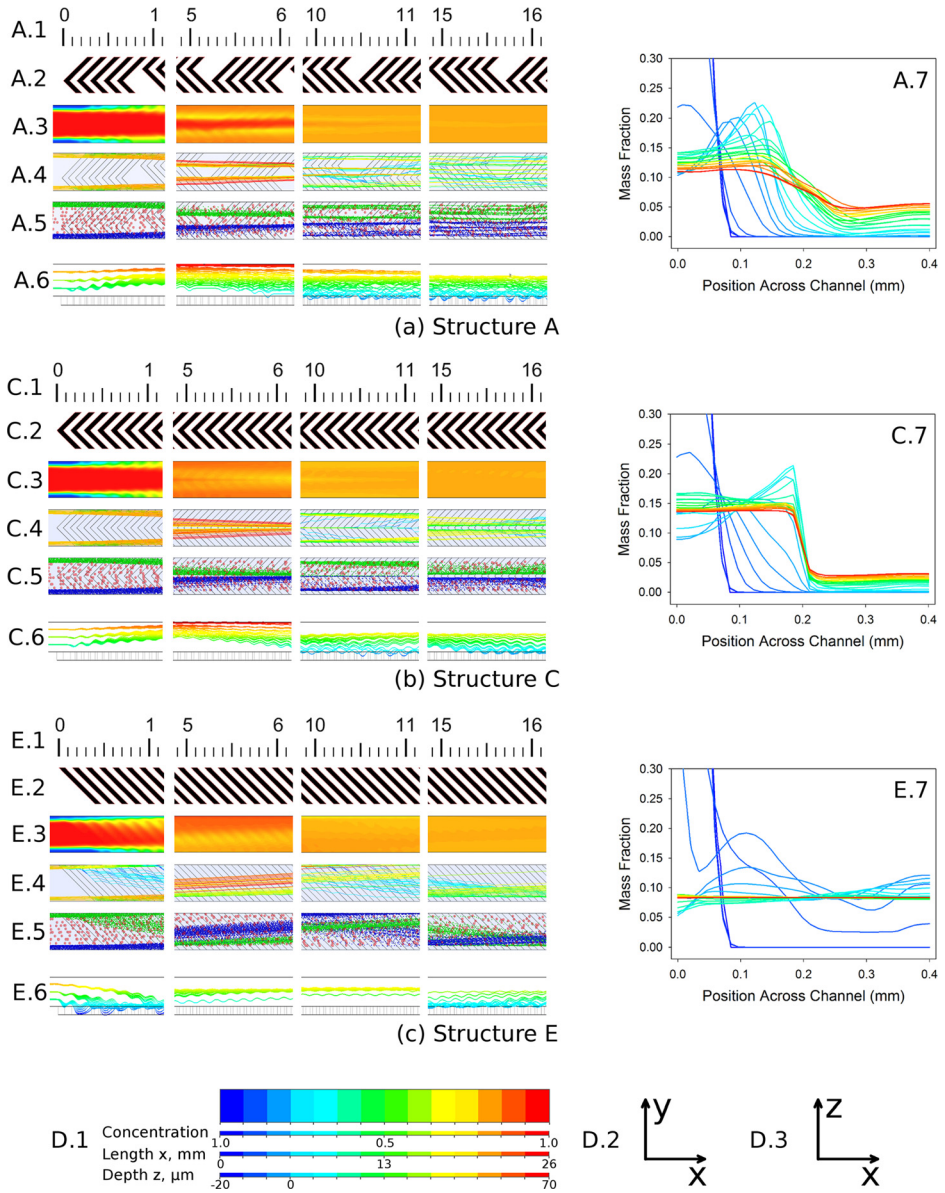

FIG. 5. (a)–(c) Simulation results for three of the main structures. Feature 1 (A.1, C.1, E.1) shows the distance along the channel in mm. Feature 2 shows the structure being simulated. Feature 3 shows the concentration profile across the channel. Feature 4 shows the flow trajectory, while feature 5 shows a visualisation of droplets flowing down the channel, with green and blue representing the secondary flow of emulsified cross linker, and red being the protein droplets. Features 2–5 show a top view of the channel (D.2). Feature 6 shows a side view of the flow trajectory (D.3). Feature 7 shows concentration profiles of the secondary emulsion as one travels down the lengths of the channel (length x). D.1 defines the colours used in the simulation.

emulsion across the centre line, while also resulting in a rapid mixing of secondary and primary emulsions. In order to determine whether this model could be successfully utilised to design variant structures, the eight simulated structures were manufactured and experimentally evaluated for a comparison to be made.

Structures were designed using a standard CAD package and manufactured utilising a soft lithography technique described extensively in the literature.[36,37] Briefly, a transparency mask is printed from the CAD design. SU-8, a negative photo resist, is spin coated onto a silicon carrier wafer and soft baked. The SU-8 layer is illuminated by i-line UV light through the mask. The UV light cross links the SU-8, and after appropriate post processing, results in a permanent

micro structure remaining on the carrier wafer. This acts as a mould for the production of a negative form from PDMS (polydimethylsiloxane), which is removed from the wafer. Entry and exit holes for the fluids are punched into the PDMS film which is then permanently bonded onto a glass substrate.

It should be noted that the structures formed from SU-8 are positive reliefs, so that after moulding, the rib-like micro-structures are eventually manufactured into the PDMS micro-channel floor. Figure 6 shows photographs of the structures in PDMS after manufacturing. The actual dimensions of the grooves formed by the positive structures are 81 μm, with the distances between grooves being 68 μm. Note that this is due to the fact that the manufacturing process results in slightly oversized structures. The main channel dimensions (width $\times$ depth $= 400\,\mu\text{m} \times 70\,\mu\text{m}$) are unchanged for channels with and without structures. The structures themselves have a height of 20 μm.

All experiments were done at flow rates of 4 μl/min for the dispersed aqueous phase (flowing into junction A, Figure 4), 1 μl/min for the continuous oil phase (flowing into alternate sides of junction A) and 1 μl/min for the cross linker micro emulsion (flowing into junction B). A specific application example, with the final goal of producing self immobilised enzymes, was chosen to test the simulation results. Immobilisation of enzymes is important when considering their operational stability and recovery and recycling. Self immobilisation allows for higher volumetric yields, and has thus been studied in great detail.[38] Microfluidic methods allow for the production of these self-immobilised enzymes, where the resultant particle size is highly controllable and monodisperse.

The dispersed phase was prepared by dissolving 240 mg/ml partially purified lipase (Pseudomonas Fluorencens Lipase AK "Amano") and 60 mg/ml of lyophilised BSA in 250 mM tris-HCl buffer solution (pH 7.2). The continuous phase was prepared by dissolving 3% (m/m) Span 80 surfactant in mineral oil. The cross-linker reagent was prepared by reacting 100 μl of glutaraldehyde (GLA—25% m/v) solution with 120 μl of ethylene diamine (EDA—0.33 M, pH 6) solution containing Triton X-100 (9% m/v) surfactant for 45 min. A further 100 μl GLA solution was added into the mixture. The reacted mixture was then emulsified by magnetic stirring in 1.2 ml of mineral oil containing 5% m/m Span 80 for 15 min.[39] All solutions were introduced by means of syringe pumps. The droplet size of the cross linker emulsion was of the order of 1 μm diameter. Droplets forming in the flow focusing junction were of the order of 50 μm diameter. Droplet diameters were measured with the aid of optical microscopes. Coalescence of the pre-emulsion is by collision with the larger droplets. Reynold's numbers for the continuous oil phase in the serpentine channels were of the order of 0.1. This corresponds to the typical Reynold's number values found in literature for these devices, where values are typically reported $\text{Re} < 100$, and often $\text{Re} \ll 1$.[15,16,20]

The activity of the resultant immobilised enzyme particles was determined in the hydrolysis of p-nitrophenyl esters, p-nitrophenyl palmitate (PNPP), and p-nitrophenyl butyrate (PNPB) to

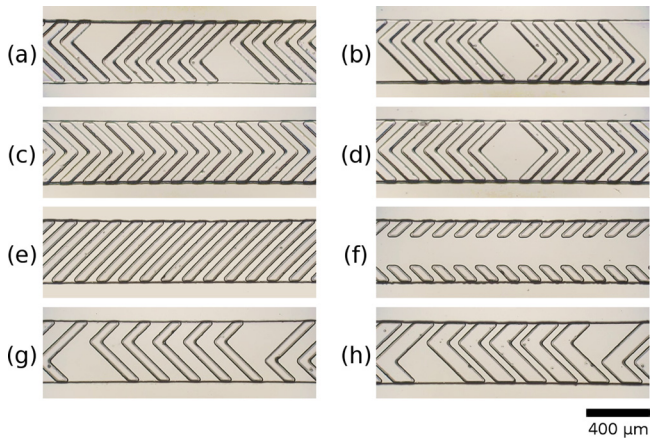

FIG. 6. Photographs of the final manufactured structures in PDMS.

p-nitrophenol and an aliphatic carboxylic acid. The calorimetric assays were performed using a PowerWave HT Microplate Spectrophotometer (BioTek Instruments) with a temperature-controlled microtitre plate reader. The kinetic measurements were conducted at wavelength of 410 nm and temperature of 35 °C. Enzyme activity (U) is the amount of enzyme necessary to produce 1 μmol of p-nitrophenol per minute and the specific activity is activity per unit mass of protein in solution (U/mg). Activity retention was determined as percentage of the specific activity of the immobilised enzyme to the specific activity of the free enzyme in solution.

III. RESULTS

Figure 7 compares numerical simulations and experiments (videos of these experiments are available in the supplementary material[40]). Experimental images of the 26 mm long channel are created by stitching together high resolution images taken from these videos. For the eight structures shown, a remarkably close correlation is achieved between simulation and experiment, confirming the laminar nature of the flows and the adequacy of the mesh used for the simulations. Figures 7(i) and 7(j) show structures A and C mixing when the primary droplets are also present in the channel. It is clear that the presence of the droplets allows for a further increase in mixing and that larger and smaller droplets both follow the flow lines.

While it is difficult to accurately determine the point where complete mixing has taken place (we used a visual queue), the trend of mixing is clear, and it is immediately obvious which structures are effective and which not. The estimated mixing lengths and times are reported in Table I. As expected, structure F allows for little mixing to occur as the structures do not extend into the middle of the channel, and thus the emulsions are effectively kept separate. These structures may find application where, for example, dispersion of the outer emulsion is required without direct contact with the inner emulsion. The concentration of emulsion can also be varied in this way. Structures A–D, G, and H all showed rapid mixing, although those with similar dimensions for the in-channel ribs and distance between ribs ($p = q$) showed faster mixing. Structure A showed complete mixing within 10.8 mm, and this structure was utilised for the further work reported.

It is also interesting to note that the larger particles formed can be controlled by reversing the direction of the structures (structures B and D). Structures pointing towards the oncoming droplets tend to focus the droplets towards the centre of the channel, while structures pointing in the direction of the flow tend to defocus the droplets and push them towards the channel walls. This observation has not been studied in detail here, but could also be useful to further enhance the mixing and coalescence of the droplets.

Figure 8 compares the mixing that occurs in a microfluidic device with ribs (structure A) with channels containing no ribs (serpentine channels as shown in Figure 4).

After a length of 104 mm (26 s), it is still apparent from the light colour of the centre of the channel that mixing is not complete (Figure 8(e)). This presents a problem, as droplets from the cross linker (secondary) emulsion require a certain residence time to effectively coalesce with the larger primary droplets. Where there are no structures, mixing only occurs shortly before the droplets exit the device. In the case of the structured channels, a residence length of 96 mm (24 s) is provided after complete mixing has occurred, and before exit of the droplets from the device.

When the flow rate of the aqueous phase is increased to 10 μl/min, complete mixing is achieved after 17 mm with structure A, which still represents a considerable benefit when compared to channels without structures, and suggests that these structures could also be successfully utilised in a scaled-up operation. These increased flow rates were also simulated and compared closely with the experimental results.

Figure 9 shows resulting droplets product which have traversed the entire length of the serpentine channel without structures. Due to the laminar nature of the flow, the primary flow droplets either experience a long period of mixing (where the droplets move close to the channel walls and are in contact with concentrated secondary emulsion) or very little mixing (where the droplets move in the channel centre and do not contact with the smaller emulsion droplets).

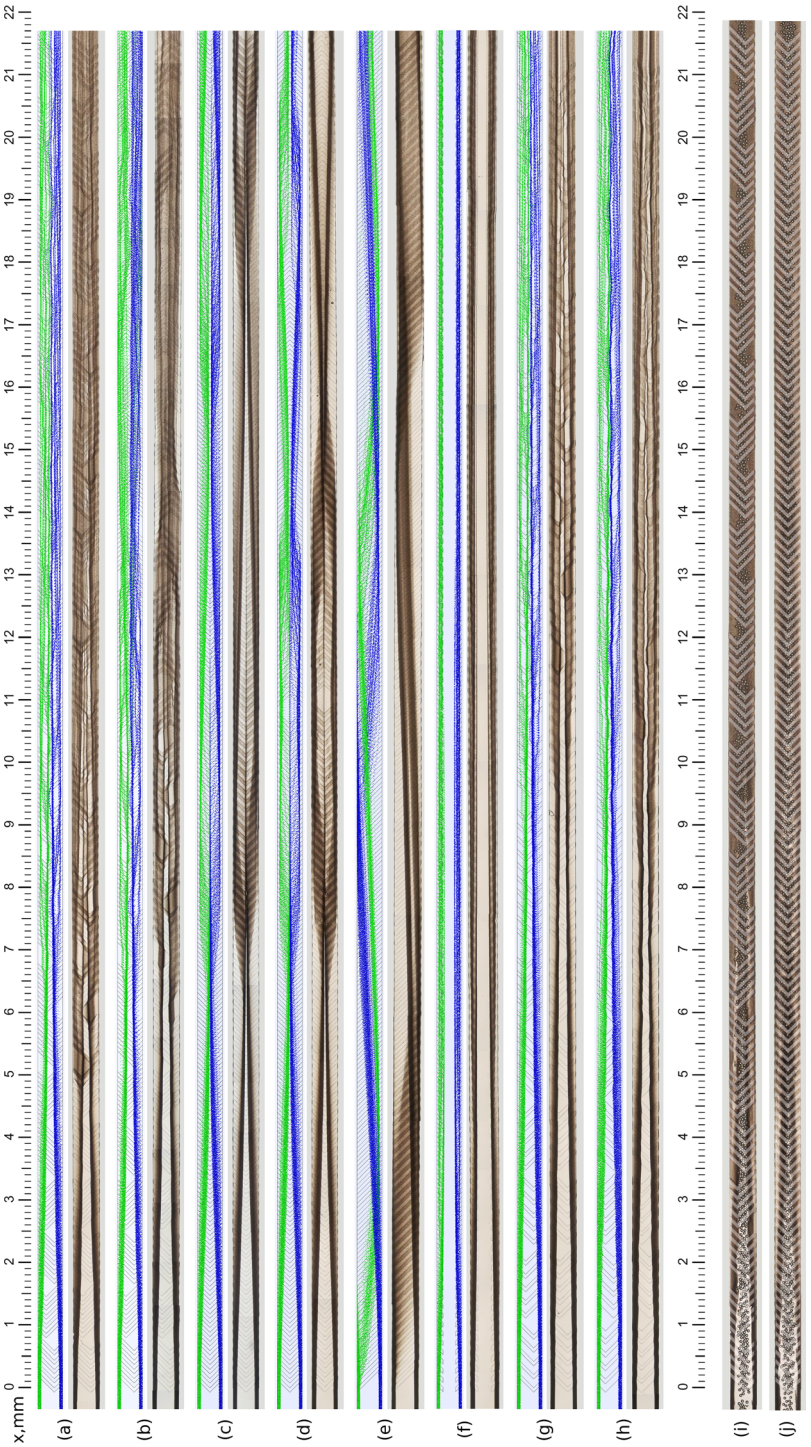

FIG. 7. Simulated and experimental comparisons for each of the structures A–H ((a)–(h)). Blue and green colours represent simulated flow trajectories of the secondary flow, while the brown colour shows photographs of the actual experiment. (i) and (j) show experimental results of mixing with structures A and C when the primary emulsion droplets are present, and a direct comparison can be made with (a) and (c), respectively, to show a further decrease in mixing time. Videos of each experiment can be found online in the supplementary material.[40]

TABLE I. Mixing lengths and times for complete mixing of the two emulsions. Total channel length is 110 mm (Figure 2) over which little mixing is achieved without structures and this value is used to calculate improvement factor when structures are introduced. These tests were carried out in straight channels with a length of 26 mm.

Structure	Mixing length (mm)	Factor	Mixing time (s)	Structure	Mixing length (mm)	Factor	Mixing time (s)
A	10.8	10.2×	2.7	E	>26	<4.2×	>6.5
B	13.1	8.4×	3.3	F	>26	<4.2×	>6.5
C	13.2	8.3×	3.3	G	16.5	6.7×	4.1
D	15.2	7.2×	3.8	H	17.6	6.3×	4.4

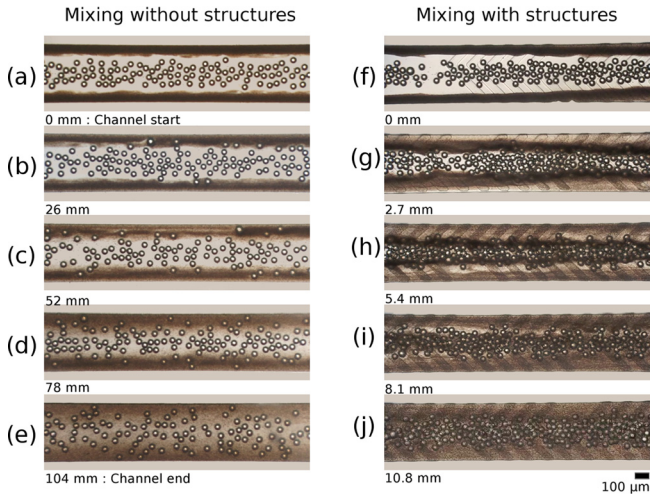

FIG. 8. Series of photographs showing different stages of mixing in channels with and without structures.

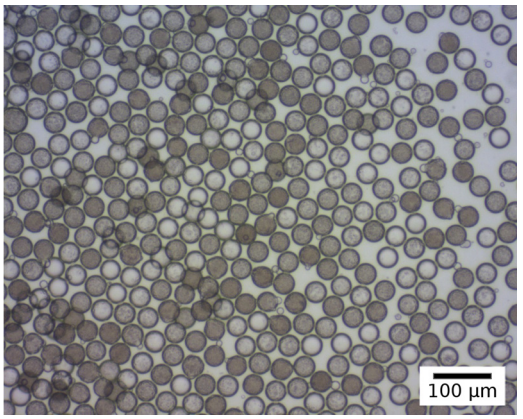

FIG. 9. Photograph showing the droplets formed when there are no structures in the channels.

This leads to inconsistent cross linking, which is not desirable, and can be seen from the varying colour intensity of the droplets. To further characterise this difference in cross-linking a grey scale analysis of the images was performed. Results were binary, with insufficient intermediate results, so that further investigation of this method was stopped. An experimental analysis, shown in Figure 10, was investigated whereby the flow from the channel was collected at five different outputs, representing different positions across the channel. Enzymatic activity retention was measured for each of these outputs, resulting in maximum activity retention in the regions represented by Figures 10(b) and 10(d). Regions (a) and (e) resulted in over

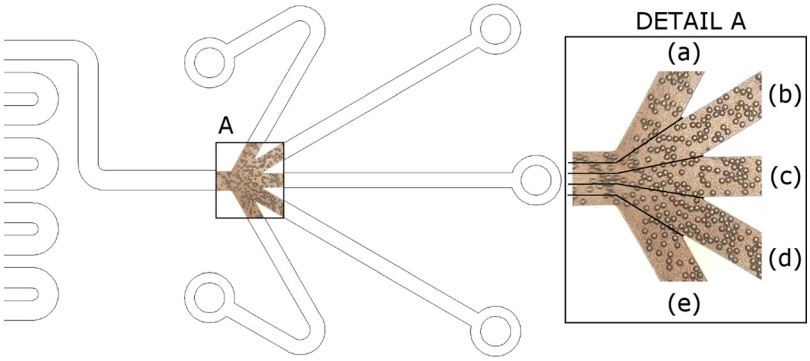

FIG. 10. Schematic showing different collecting regions (measured across the width of the channel) for the droplets, (a) 0–80 μm, 26% activity retention, (b) 80–160 μm, 51%, (c) 160–240 μm, 17%, (d) 240–320 μm, 73%, and (e) 320–400 μm, 27%.

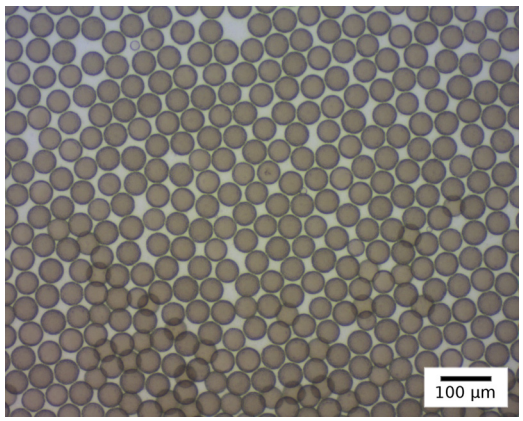

FIG. 11. Photograph showing droplets formed when structures are utilised to mix reagents well before the device exit.

cross-linked particles, while the central region (c) resulted in under cross-linked particles. Both of these cases result in significantly less activity retention.

In contrast to this, Figure 11 shows the results of droplet flow in channels with structures. All droplets experience a long and equal period of mixing and coalescence, with the result that cross linking is robust and the droplets formed have very similar reagent concentrations. This consequently leads to consistent particle formation, with activity retentions in the region of 60%.

IV. DISCUSSION

We have shown the advantages which are gained by introducing structures into microfluidic channels when two emulsions (with different droplet sizes) need to be rapidly mixed.

Mixing can occur within a distance that is at least 10× shorter than that achieved without structures, and this, in turn, allows for a longer residence time in the microfluidic channel, allowing for the required coalescence of smaller droplets with larger droplets (see Table I).

We have shown one application, namely, the introduction of secondary cross linker into the bigger droplets, where it is advantageous to utilise this method. The introduction of a cross linking agent (glutaraldehyde) into the larger enzyme droplets has resulted in the successful manufacture of self-immobilised enzyme particles.

Many other applications will also benefit. As an example, the introduction of blood staining reagents into blood samples could utilise this method for point-of-care applications where rapid mixing is advantageous.

ACKNOWLEDGMENTS

The authors wish to thank the Technology Innovation Agency, Department of Science and Technology (South Africa) and the BMBF (Germany) for financial support. J.G.K. is also thankfully supported by the ERC under Contract No. 290586 (NMCEL). Louis Fourie is thanked for manufacturing the devices for testing.

[1]N.-T. Nguyen and Z. Wu, J. Micromech. Microeng. **15**, R1 (2005).
[2]J. M. Ottino and S. Wiggins, Philos. Trans. R. Soc. London, Ser. A **362**, 923 (2004).
[3]C.-Y. Lee, C.-L. Chang, Y.-N. Wang, and L.-M. Fu, Int. J. Mol. Sci. **12**, 3263 (2011).
[4]K. Sritharan, C. J. Strobl, M. F. Schneider, A. Wixforth, and Z. Guttenberg, Appl. Phys. Lett. **88**, 054102 (2006).
[5]G. G. Yaralioglu, I. O. Wygant, T. C. Marentis, and B. T. Khuri-Yakub, Anal. Chem. **76**, 3694 (2004).
[6]C.-K. Chen and C.-C. Cho, J. Colloid Interface Sci. **312**, 470 (2007).
[7]H. Mao, T. Yang, and P. S. Cremer, J. Am. Chem. Soc. **124**, 4432 (2002).
[8]H. H. Bau, J. Zhong, and M. Yi, Sens. Actuators, B **79**, 207 (2001).
[9]A. E. Kamholz, B. H. Weigl, B. A. Finlayson, and P. Yager, Anal. Chem. **71**, 5340 (1999).
[10]R. F. Ismagilov, A. D. Stroock, P. J. A. Kenis, G. Whitesides, and H. A. Stone, Appl. Phys. Lett. **76**, 2376 (2000).
[11]J. Melin, G. Gimenéz, N. Roxhed, W. van der Wijngaart, and G. Stemme, Lab Chip **4**, 214 (2004).
[12]R. H. Liu, M. A. Stremler, K. V. Sharp, M. G. Olsen, J. G. Santiago, R. J. Adrian, H. Aref, and D. J. Beebe, J. Microelectromech. Syst. **9**, 190 (2000).
[13]H. M. Xia, C. Shu, S. Y. M. Wan, and Y. T. Chew, J. Micromech. Microeng. **16**, 53 (2006).
[14]C.-C. Hong, J.-W. Choi, and C. H. Ahn, Lab Chip **4**, 109 (2004).
[15]E. Biddiss, D. Erickson, and D. Li, Anal. Chem. **76**, 3208 (2004).
[16]A. D. Stroock and G. M. Whitesides, Acc. Chem. Res. **36**, 597 (2003).
[17]H. Wang, P. Iovenitti, E. Harvey, and S. Masood, J. Micromech. Microeng. **13**, 801 (2003).
[18]M. S. Williams, K. J. Longmuir, and P. Yager, Lab Chip **8**, 1121 (2008).
[19]S. P. Kee and A. Gavriilidis, Chem. Eng. J. **142**, 109 (2008).
[20]A. D. Stroock, S. K. W. Dertinger, A. Ajdari, I. Mezic, H. A. Stone, and G. M. Whitesides, Science **295**, 647 (2002).
[21]S.-Y. Teh, R. Lin, L.-H. Hung, and A. P. Lee, Lab Chip **8**, 198 (2008).
[22]A. Huebner, S. Sharma, M. Srisa-Art, F. Hollfelder, J. B. Edel, and A. J. Demello, Lab Chip **8**, 1244 (2008).
[23]B. Kintses, L. D. van Vliet, S. R. A. Devenish, and F. Hollfelder, Curr. Opin. Chem. Biol. **14**, 548 (2010).
[24]E. Tumarkin and E. Kumacheva, Chem. Soc. Rev. **38**, 2161 (2009).
[25]S. Seiffert, Macromol. Rapid Commun. **32**, 1600 (2011).
[26]T. Thorsen, R. W. Roberts, F. H. Arnold, and S. R. Quake, Phys. Rev. Lett. **86**, 4163 (2001).
[27]S. L. Anna, N. Bontoux, and H. A. Stone, Appl. Phys. Lett. **82**, 364 (2003).
[28]H. Song, D. L. Chen, and R. F. Ismagilov, Angew. Chem. Int. Ed. Engl. **45**, 7336 (2006).
[29]N. Bremond, A. Thiam, and J. Bibette, Phys. Rev. Lett. **100**(2), 024501 (2008).
[30]L. Mazutis, J. Baret, and A. D. Griffiths, Lab Chip **9**, 2665 (2009).
[31]H. Gu, C. U. Murade, M. H. G. Duits, and F. Mugele, Biomicrofluidics **5**, 11101 (2011).
[32]P. Carreras, S. Mohr, P. Fielden, and N. Goddard, in *Proceedings of the 12th International Conference on Miniaturized Systems for Chemistry and Life Sciences—MicroTAS 2008* (Chemical and Biological Microsystems Society, 2008), pp. 1393–1395.
[33]V. Chokkalingam, S. Herminghaus, and R. Seemann, Appl. Phys. Lett. **93**, 254101 (2008).
[34]S. Choi and J.-K. Park, Lab Chip **7**, 890 (2007).
[35]C.-H. Hsu, D. Di Carlo, C. Chen, D. Irimia, and M. Toner, Lab Chip **8**, 2128 (2008).
[36]Y. Xia and G. M. Whitesides, Angew. Chem. Int. Ed. **37**, 550 (1998).
[37]G. M. Whitesides, E. Ostuni, S. Takayama, X. Jiang, and D. E. Ingber, Annu. Rev. Biomed. Eng. **3**, 335 (2001).
[38]R. A. Sheldon, Adv. Synth. Catal. **349**, 1289 (2007).
[39]M. B. Mbanjwa, H. Chen, and K. Land, in *Proceedings of the 17th International Conference on Miniaturized Systems for Chemistry and Life Sciences—MicroTAS 2013* (Chemical and Biological Microsystems Society, 2013), pp. 1248–1250.
[40]See supplementary material at http://dx.doi.org/10.1063/1.4894498 for videos showing experiments performed for each of the structures and for the case of no structures.